Traveling Wave Fault Location in Protective Relays: Design, Testing, and Results

Stephen Marx
Bonneville Power Administration

Brian K. Johnson
University of Idaho

Armando Guzmán, Veselin Skendzic, and Mangapathirao V. Mynam
Schweitzer Engineering Laboratories, Inc.

Traveling Wave Fault Location in Protective Relays: Design, Testing, and Results

Stephen Marx, *Bonneville Power Administration*
Brian K. Johnson, *University of Idaho*
Armando Guzmán, Veselin Skendzic, and Mangapathirao V. Mynam, *Schweitzer Engineering Laboratories, Inc.*

Abstract—**Faults in power transmission lines cause transients that travel at a speed close to the speed of light and propagate along the line as traveling waves (TWs). This paper shows how these transients can be measured in a protective relay and used to enhance its fault locating function. The TW-based fault locating function in a protective relay takes advantage of the internal protection elements, the communications channel to the remote terminal, and Global Positioning System-based time synchronization. This approach provides accurate fault location estimation for transmission lines automatically within a couple of seconds after the fault. The TW fault locator within the relay uses conventional current transformer measurements and does not require any additional wiring or special installation considerations. These relays detect internal line faults and use TW- and impedance-based algorithms to optimize the estimation and reporting of the fault location. The TW- and impedance-based algorithms complement each other to provide accurate fault location estimation for all internal faults, independent of the fault incidence angle. This paper provides a tutorial on TW fault location and describes a TW fault locating algorithm that uses time-synchronized measurements of the TW currents at the line terminals to determine the fault location. The proposed implementation is suitable for line terminals with one or two breakers. The paper also discusses methods for testing the TW fault locating algorithm using a playback system and a hardware model that mimics a transmission line. The paper presents the details and experiences of a field application of these relays on a high-voltage transmission line.**

I. INTRODUCTION

The Bonneville Power Administration (BPA) has been using traveling wave (TW) technology to locate faults in their extra-high voltage (EHV) transmission networks since the 1950s [1]. In the 1960s and 1970s, BPA installed an automated fault locating system that used microwave communications to send the TW arrival information to the remote terminal for fault location estimation [2]. References [3] and [4] describe the development and field evaluation of the performance of a digital fault locator for high-voltage direct current (HVDC) lines that uses voltage and current measurements from one line terminal to estimate the fault location. Using voltage and current measurements, we can calculate incident and reflected waves. Applications based on incident waves are immune to the effects caused by termination impedances. In 1987, BPA started to use Global Positioning System (GPS) time information to measure the arrival of the TWs [5].

Later on, utilities like BPA used dedicated TW-based fault locating devices that sample the currents or voltages at sampling rates greater than 1 MHz [6]. Some of these devices also include fault disturbance recording and are capable of reporting accurate fault location results [7].

Numerical protective relays include fault location estimation algorithms based on the line impedance and voltage and current measurements. In most applications, these relays only use measurements from the local terminal. Some relays also use information from the remote terminal to estimate the fault location. Using information from the local and remote terminals minimizes errors due to mutual coupling with adjacent lines, system nonhomogeneity, and fault resistance [8] [9]. In some applications, such as series-compensated lines, the impedance-based fault locating methods are challenged and utilities require more accurate estimation than traditional relays provide.

This paper discusses the basic principles of TWs, a protective relay that estimates fault location using TW information, and the benefits of having TW fault location estimation within a protective relay. The paper also describes how to test the TW fault locating system using low-energy analog signals and an analog transmission line model. We also share the field experiences from an installation on a BPA 161 kV transmission line.

II. OVERVIEW OF TRAVELING WAVES IN TRANSMISSION LINES

A fault on a transmission line generates TWs that propagate from the fault location to the line terminals with a propagation velocity that depends on the inductance and capacitance of the line. Fig. 1 shows the equivalent circuit of a segment with length Δx of a two-conductor transmission line. The circuit includes the resistance R, inductance L, conductance G, and capacitance C of the line in per unit of the total line length [10].
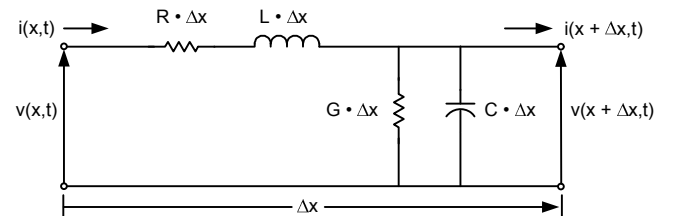

Fig. 1.   Equivalent circuit of a segment of a two-conductor transmission line.

We use Kirchhoff's voltage law, shown in (1), and Kirchhoff's current law, shown in (2), to relate the voltages and currents at locations x and x+Δx.

$$v(x,t) = R \bullet \Delta x \bullet i(x,t)$$
$$+ L \bullet \Delta x \frac{\partial i(x,t)}{\partial t} + v(x + \Delta x, t) \tag{1}$$

$$i(x,t) = G \bullet \Delta x \bullet v(x + \Delta x, t)$$
$$+ C \bullet \Delta x \frac{\partial v(x + \Delta x, t)}{\partial t} + i(x + \Delta x, t) \tag{2}$$

Equations (3) and (4) determine the voltage and current as a function of x and time for the two-conductor transmission line in the time domain as the length of the segment Δx approaches zero.

$$\frac{\partial v(x,t)}{\partial x} = -R \bullet i(x,t) - L \frac{\partial i(x,t)}{\partial t} \tag{3}$$

$$\frac{\partial i(x,t)}{\partial x} = -G \bullet v(x,t) - C \frac{\partial v(x,t)}{\partial t} \tag{4}$$

We differentiate (3) with respect to x and (4) with respect to t to obtain (5) and (6), respectively.

$$\frac{\partial^2 v(x,t)}{\partial x^2} = -R \frac{\partial i(x,t)}{\partial x} - L \frac{\partial^2 i(x,t)}{\partial x \partial t} \tag{5}$$

$$\frac{\partial^2 i(x,t)}{\partial x \partial t} = -G \frac{\partial v(x,t)}{\partial t} - C \frac{\partial^2 v(x,t)}{\partial t^2} \tag{6}$$

We substitute $\frac{\partial i(x,t)}{\partial x}$ from (4) and $\frac{\partial^2 i(x,t)}{\partial x \partial t}$ from (6) into (5) to obtain the voltage wave equation shown in (7).

$$\frac{\partial^2 v(x,t)}{\partial x^2} = LC \frac{\partial^2 v(x,t)}{\partial t^2}$$
$$+ (RC + GL) \frac{\partial v(x,t)}{\partial t} + GR \bullet v(x,t) \tag{7}$$

Similarly, we differentiate (3) with respect to t and (4) with respect to x to obtain (8) and (9), respectively.

$$\frac{\partial^2 v(x,t)}{\partial x \partial t} = -R \frac{\partial i(x,t)}{\partial t} - L \frac{\partial^2 i(x,t)}{\partial t^2} \tag{8}$$

$$\frac{\partial^2 i(x,t)}{\partial x^2} = -G \frac{\partial v(x,t)}{\partial x} - C \frac{\partial^2 v(x,t)}{\partial x \partial t} \tag{9}$$

We substitute $\frac{\partial v(x,t)}{\partial x}$ from (3) and $\frac{\partial^2 v(x,t)}{\partial x \partial t}$ from (8) into (9) to obtain the current wave equation shown in (10).

$$\frac{\partial^2 i(x,t)}{\partial x^2} = LC \frac{\partial^2 i(x,t)}{\partial t^2}$$
$$+ (RC + GL) \frac{\partial i(x,t)}{\partial t} + GR \bullet i(x,t) \tag{10}$$

Equations (7) and (10) determine how the voltage and current waves propagate along a two-conductor transmission line.

To analyze the voltage and current TWs in multiphase transmission lines, we used an Electromagnetic Transients Program (EMTP) that models transmission lines considering the changes in the conductor resistance and inductance due to skin effect [11] [12] [13]. Fig. 2 shows how the current waves propagate across a 400 kV line in response to a nominal voltage step change on A-phase and B-phase at the sending end (the step change occurs at t = 0).
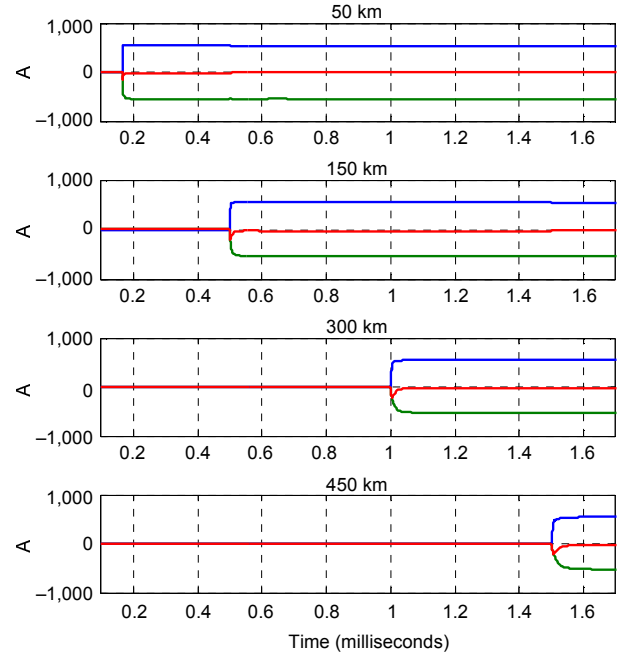

Fig. 2. Current waves at 50, 150, 300, and 450 kilometers traveling on a 400 kV line for a nominal voltage step change at the sending end, where A-phase is green, B-phase is blue, and C-phase is red.

III. TRAVELING WAVE FAULT LOCATION FOR TWO-TERMINAL LINES

TW-based fault location provides better accuracy relative to impedance-based fault locating methods. Single end (Type A) and double end (Type D) are the two most common methods for computing fault location using TWs [1]. Type A uses the time difference between the first arrived wave and the successive reflections from the fault location to compute the fault location. This method is appealing because it only depends on local information; therefore, it does not require a communications channel. However, identifying the reflections is a major challenge. The reflections can arrive from the fault location, from the remote terminal, or from behind the local terminal. Accurately identifying the reflection from the fault location poses a challenge for single-end TW-based fault location, especially on ac transmission lines. The double-end method overcomes the challenge of identifying the reflections from the fault but requires the TW information from the remote terminal. This Type D method uses the time difference between the first arrived TWs captured at both terminals along with the line length and the wave propagation velocity to compute the fault location. Fig. 3 shows the waves propagating to Terminals A and B following a fault condition on a transmission line.
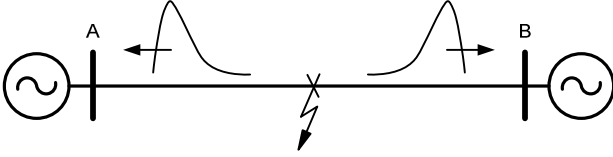

Fig. 3. TWs propagating to Terminals A and B.

Measurement devices at the line terminals detect the TWs and accurately time-stamp the arrival of the wave using a common time reference (e.g., IRIG-B or IEEE 1588). The typical time-stamping accuracy is better than 1 microsecond. The TW-based fault location is computed using (11).

$$\text{TWFL} = \frac{\text{LL} + \left(\text{TwaveA} - \text{TwaveB}\right) \bullet c \bullet \text{LPVEL}}{2} \quad (11)$$

where:

TWFL is the TW-based fault location.

LL is the line length.

TwaveA is the TW arrival time recorded at Terminal A.

TwaveB is the TW arrival time recorded at Terminal B.

c is the speed of light.

LPVEL is the propagation velocity of the TW in per unit of the speed of light.

The TW propagation velocity is a key parameter in the fault location calculation and is typically obtained from line parameter estimation programs. We can also estimate propagation velocity using TW measurements with the following:

- Local TW information recorded during line or reactor energization tests.
- Local and remote TW information recorded during external faults.

Voltage and/or current measurements capture the TWs. The adequate frequency bandwidth of current transformers (CTs) makes current TWs better suited for this application than voltage TWs measured at the secondary terminals of the step-down transformer of the capacitance coupled voltage transformer (CCVT) [14]. Typical installations have communications between the substation and the control center, where computer-based analysis tools retrieve the TW information captured at the line terminals and compute the fault location. In this paper, we discuss installations where protective relays exchange TW information obtained from the phase currents and automatically calculate the fault location at the line terminals within a couple of seconds after the fault.

IV. TW FAULT LOCATION IN PROTECTIVE RELAYS

A. Benefits of TW Fault Location in a Protective Relay

Numerical protective relays have included fault location estimation based on voltage and current measurements and line impedance since 1982 [15] [16]. These relays use voltage and current measurements acquired at the local terminal and report the fault location estimation results at the substation and the control center through automessaging right after the occurrence of a fault. While this approach provides estimations within 2 percent of the line length, there are cases where mutual coupling, fault resistance, and system nonhomogeneity can cause large errors. In these cases, the impedance-based fault locating methods in protective relays can be improved using local and remote (double-end) measurements [8] [9] [17].

Impedance-based fault location estimation requires the presence of the fault for a couple of cycles to provide accurate results. While this requirement is not an issue in subtransmission network applications, it can be an issue in EHV and ultra-high voltage (UHV) applications where faults are sometimes cleared in less than two cycles. Furthermore, these impedance-based estimation methods might not be applicable to lines with series compensation or lines close to series compensation due to subsynchronous oscillations, voltage inversion, and so on. Because of the importance of locating faults to avoid fault reoccurrences and the high cost associated with finding line faults, utilities require accurate fault locating devices for all applications. For this reason, some utilities have installed dedicated devices that detect the time of arrival of TWs at the line terminals and estimate the fault location using this information [6] [18]. While these devices provide more accurate fault location estimation than relays that use impedance-based methods to estimate the fault location, there are cases where they cannot estimate the fault location when faults occur at the voltage zero crossing.

Protective relays that include both impedance-based and TW-based fault location have the advantage of providing fault location even in cases where the TW amplitude is too low for reliable detection (e.g., faults that occur at voltage zero). In these cases, the relays estimate the fault location using line impedance and local and remote voltage and current measurements. If the remote measurements are not available, the relay estimates the fault location using local measurements

only, thus providing robust response with the best possible accuracy under all fault conditions.

B. Relay-to-Relay Communications

The relay discussed in this paper uses a 64 kbps channel that exchanges currents for differential protection purposes. The relay takes advantage of this bandwidth and includes TW information within the data packet without affecting the performance of the differential element. The relays exchange the times of arrival of the TWs (see Fig. 4) and use this information to estimate the fault location, make the results available at the relay location, and send the results to the control center within a couple of seconds after the occurrence of the fault.
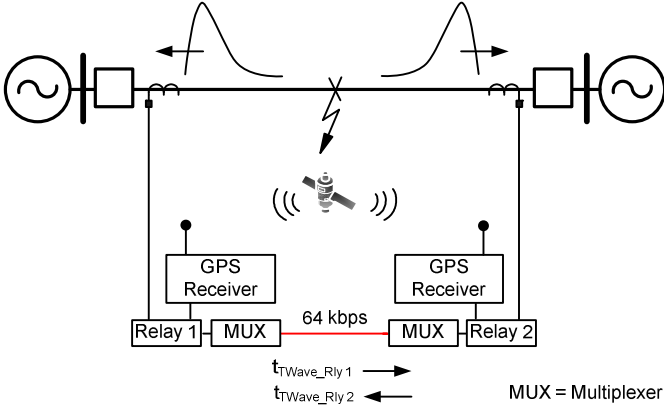
Fig. 4.   Relays exchange the time of arrival of the TW to estimate the fault location in real time.

C. Traveling Wave Measurements

High-frequency transients created by power system faults propagate at speeds that are close to the speed of light. However, high-voltage transmission lines are optimized to operate at nominal power system frequency with standard values of 50 or 60 Hz, and some of them are dc lines. Significant engineering effort is made in reducing the transmission line losses at these frequencies, with no attempt to consider their behavior at the high frequencies (0.1 to 1 MHz) that are used by TWs.

Fortunately, the physics associated with the construction of efficient high-voltage transmission lines aid with the TW propagation. For various economic, operational, and environmental reasons, high-voltage transmission lines are built as regular structures, with uniform distances among phase conductors, uniform dielectric (air), constant conductor cross section, and regular transmission tower support, as illustrated in Fig. 5. Because of all of these factors, transmission lines can transport signals well into the megahertz range. This fact has been used for a very long time and is best exemplified by the power line carrier-based communications that operate in the 100 to 600 kHz range. In addition to transmission lines with well-defined losses, TW-based fault location is further aided by the fact that power system faults generate significant amounts of energy in the frequency range of interest. This energy provides sufficient signal levels at the transmission line ends to indicate the presence of a fault on the line.
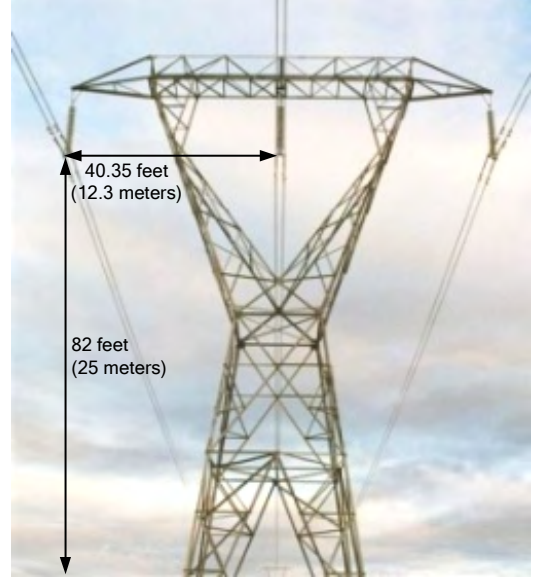

Fig. 5.   Typical high-voltage transmission tower.

Arrival of the TWs at the substations with sufficient energy is only the initial prerequisite for successful TW-based fault location. Once the waves arrive, they must be measured (extracted from the current and/or voltage measurements) and delivered to the fault location estimation algorithm. Currents and voltages on the transmission line are measured using standard CTs and voltage transformers (VTs). The responses of the CTs and VTs have been optimized for nominal frequency operation. TW signals can be measured using specialized high-frequency transducers similar to those used in high-voltage laboratories, but the high cost and custom nature of these devices make this approach impractical for wide-scale utility applications.

From the perspective of utilities, it would be ideal if the TW-based fault locating device could be installed in the substation control house using conventional wiring practices. It is also highly desirable that the new device be deployed without requiring new communications or time-synchronization infrastructure. While studying this problem, the authors decided to start by investigating the frequency response of conventional instrument transformers. We classified measurement transformers in the following subcategories.

Current transformers include:
- Conventional iron-core CTs
- Nonconventional low-energy CTs
  - Optical CTs
  - Low-power CTs
  - Rogowski coils

Voltage transformers include:
- Conventional VTs
  - CCVTs
  - Inductive VTs
  - Open magnetic core-based VTs

- Nonconventional low-energy VTs
  - High-voltage capacitive, resistive, and compensated dividers
  - Transformer bushing tap-based VTs (capacitive dividers)
  - Optical VTs

Comparison of the available technologies shows that the two most popular choices used for current and voltage measurements on high-voltage (greater than 69 kV) transmission lines are conventional CTs (freestanding or bushing design) and CCVTs.

Conventional CT construction is very simple (a toroidal core with at least one secondary winding). Conventional CTs have good high-frequency response [19]. The CT bandwidth measurement results reported in literature vary, but the common consensus is that the usable pass band (–3 dB point) easily reaches 100 kHz [19] and may often be closer to the 200 kHz [20] or 500 kHz level [21]. Measurements performed by the authors confirm these results (300 kHz, in our case), with the additional finding that the measurement bandwidth is inversely proportional to the CT ratio. Low-ratio CTs have fewer turns and lower interwinding capacitance, thus providing a larger bandwidth. This effect is especially pronounced in input CTs, which are typically used to measure currents inside the protective relay.

Fig. 6 illustrates the results obtained by using an IEC 61000-4-5-compliant test generator to inject a 2 kA (8 by 20 microseconds) pulse into the primary of the tested CT. The test setup included 70 meters of #10 (5.26 mm^2) wire that connects the protective relay to the secondary of the CT.

The results shown in Fig. 6 demonstrate that equipment that was originally built to operate at 60 Hz works very well at frequencies well beyond the original design range. The output current observed at the CT secondary terminals (the middle trace) matches the primary current measured using a high-frequency shunt (the top trace).
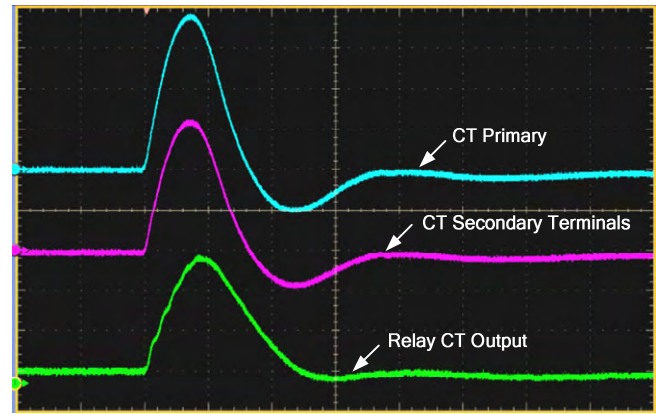

Fig. 6.   A 600:5 CT response measured using a 2 kA transient with 8 by 20 microsecond lightning surge waveform and 70 meters (230 feet) of secondary cabling.

The bottom trace shows the signal recorded at the secondary of the input CT (inside the relay). The recorded waveform is a reasonably faithful representation of the primary signal. Data obtained from this and other tests were used to design an input circuit optimized for TW applications, with the frequency response shown in Fig. 7. The response is flat up to 1 MHz with controlled high-frequency attenuation extending well into the radio frequency range.

The current measured by the relay (see Fig. 6) has additional ripple. Further simulations confirmed that this ripple was contributed by the secondary cable and that this cable does not behave as a properly terminated transmission line. At one end, the cable is connected to the CT (a current source with an impedance approaching the impedance of an infinite source), and it is terminated into a short circuit at the relay end. This configuration creates multiple reflections resulting in multiple resonances, as described in [22]. The observed ripple frequency was consistent with the length of the secondary cable.
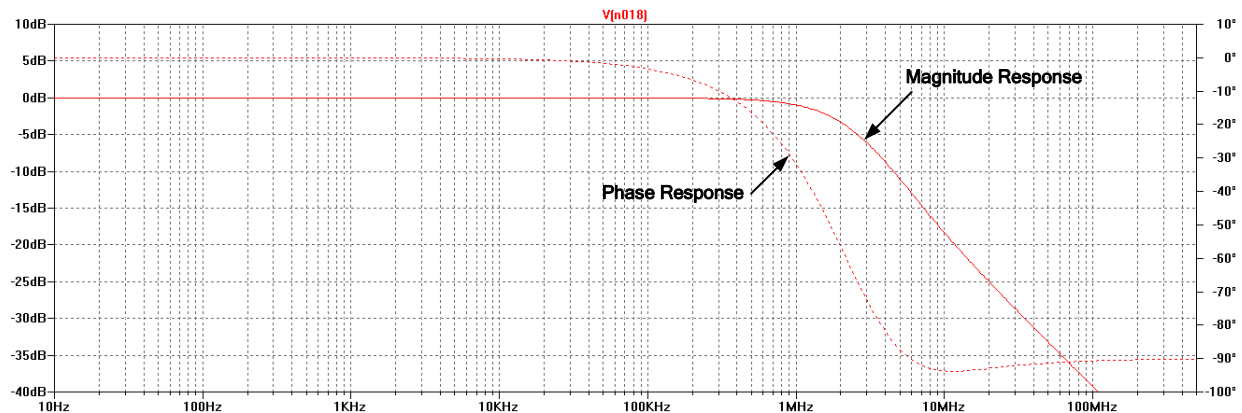

Fig. 7.   Frequency response of the relay analog circuitry (excluding anti-aliasing filter).
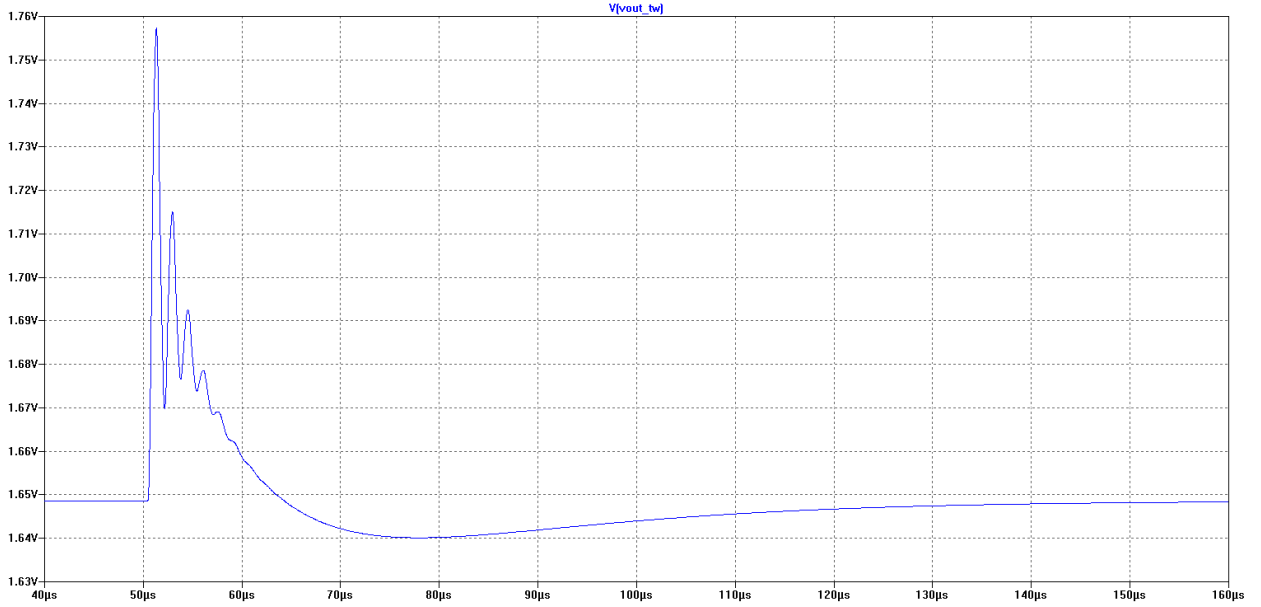
Fig. 8.   LTspice simulation showing ringing of the current signal at the relay end caused by the secondary wiring of the CT.
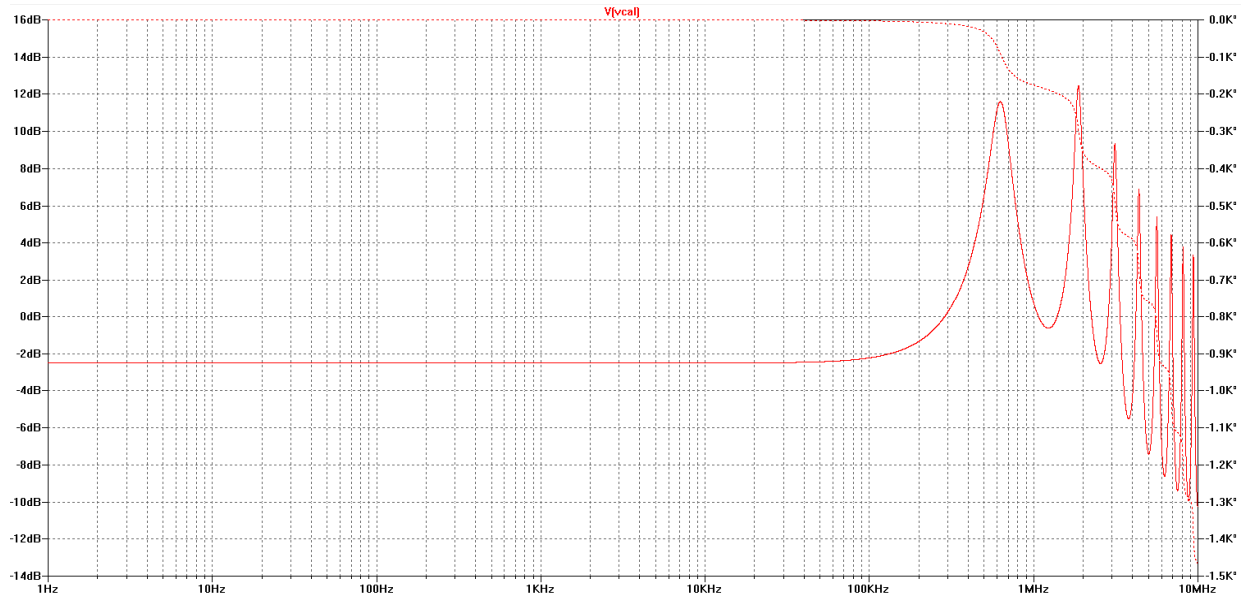

Fig. 9.   LTspice simulation showing the peaks in the frequency response caused by the secondary wiring of the CT.

Fig. 8 shows the results of an LTspice simulation that demonstrates the secondary cable ringing effects, while Fig. 9 shows the frequency response peaks caused by the same effect.

Ringing effects are present in real life, as demonstrated by the TW transient waveform shown in Fig. 10. This waveform was recorded in the field during an actual power system fault.

The TW spectral content is inherently limited by the high-frequency attenuation provided by the power system transmission line. However, as the TW transient reaches the substation (the relay location), it is capable of exciting a large number of local high-frequency resonances, which have no value for fault location estimation. Therefore, sampling frequencies found on most TW systems are normally somewhere in the 0.5 to 5 MHz range.

The TW voltage transients are also suitable for fault location estimation. Unfortunately, the quality of the measurements provided by conventional VTs is significantly inferior to that of their CT counterparts. CCVTs normally used at transmission levels are tuned to the nominal power system frequency. Although the high-frequency capacitor stacks used in these transformers are often usable up to 1 MHz, the tuning reactor eliminates the high-frequency signals, leaving only the unintended transients caused by parasitic capacitance, which tends to be different for every CCVT design [23]. Because the voltage measurements captured at the secondary terminals of the CCVT step-down transformer do not properly measure TW transients, some systems use additional high-frequency transducers mounted in series with the CCVT stack or nonconventional resistive-capacitive dividers to capture the voltage TWs.

The TW-based fault locator described in this paper does not require additional CTs or CT wiring because the relay is able to use the same current measurements for line protection and fault location estimation.

The TW-based fault locating subsystem is implemented in parallel with the conventional data acquisition chain, ensuring no interference with the mission-critical protection functions. The TW-based fault locating subsystem uses high-speed analog-to-digital (A/D) converters that sample the phase currents at 1.56 MHz and creates dedicated COMTRADE event reports that contain TW information.
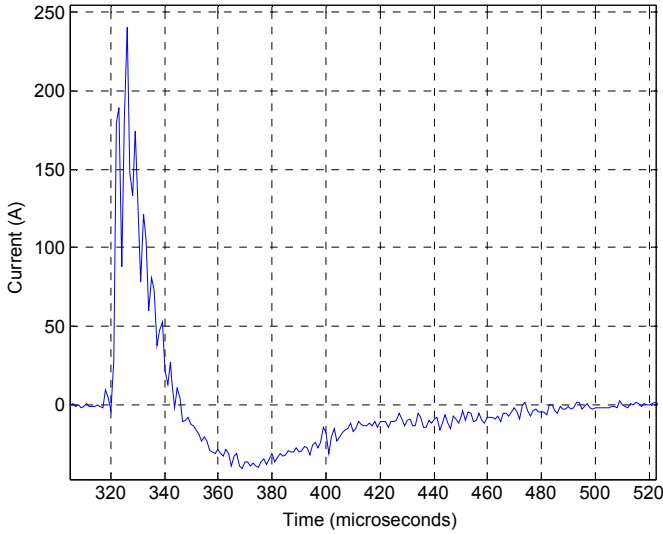
Fig. 10.   Field-recorded TW waveform showing ringing effects in an actual substation application.

D. Current Monitoring in Double-Breaker Applications

The protective relay has two sets of current inputs to measure the currents through the two breakers in breaker-and-a-half and double-breaker schemes, as Fig. 11 illustrates. This capability allows the relay to monitor the line currents based on user-programmable logic variables that select which currents to use according to the operation requirements of the power system. The fault locating algorithm uses the selected TWIA, TWIB, and TWIC currents for fault location estimation.
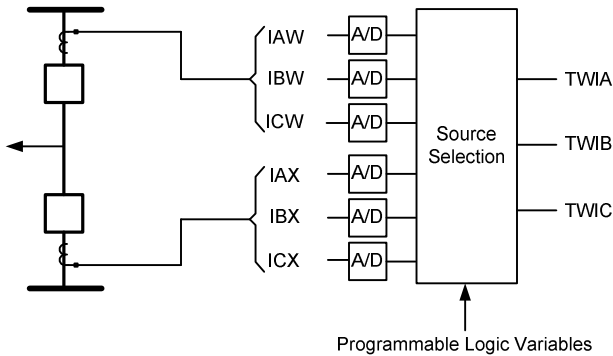

Fig. 11.   Current source selection for TW fault location in double-breaker applications.

V. Traveling Wave Testing

A. Testing Using Low-Energy Analog Signals

To verify the accuracy of the TW-based fault location estimation, we created a power system model using an EMTP. The power system model includes frequency-dependent transmission line models and effective terminal capacitance at the buses. Table I shows typical terminal capacitances for generators, transformers, and bus systems [24].

TABLE I
TYPICAL TERMINAL CAPACITANCES IN MICROFARADS (μF)

	Maximum	Minimum	Average
Hydrogenerators (Salient Poles)	0.001	0.0002	0.0006
Generators (Steam Turbine)	0.001	0.0001	0.0005
Transformers (Distribution)	0.002	0.0004	0.0010
Transformers (Power)	0.001	0.0002	0.0005
Bus Systems	0.015	0.0020	0.0050

We simulated phase-to-ground and phase-to-phase faults at known locations on a 189-mile line. We saved the current signals from both terminals (sending end and receiving end) that were sampled at a rate of 3 MHz as comma-separated value (CSV) files. We used a signal generator that is capable of playing back megahertz sampling rate data with 16-bit resolution (see Fig. 12). The signal generator plays back the CSV files via the low-energy analog (LEA) interface of the relay. Two playback units supplied the three-phase currents from each line terminal to the corresponding relays. The playback units were configured to inject the signals synchronously to both relays.
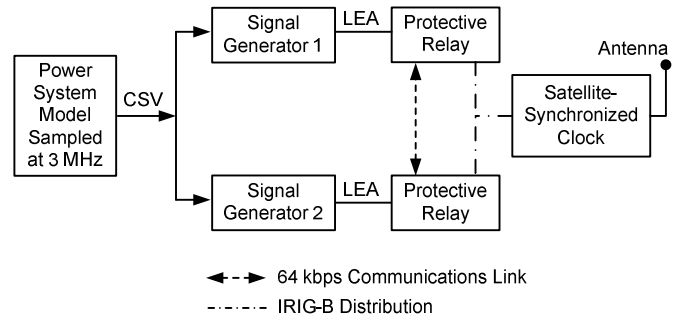

Fig. 12.   Test setup using LEA signals to test the TW fault locating system.

Fig. 13 and Fig. 14 show the phase currents at the sending and receiving terminals, respectively, for an AB fault at 160.45 miles (from the sending terminal).
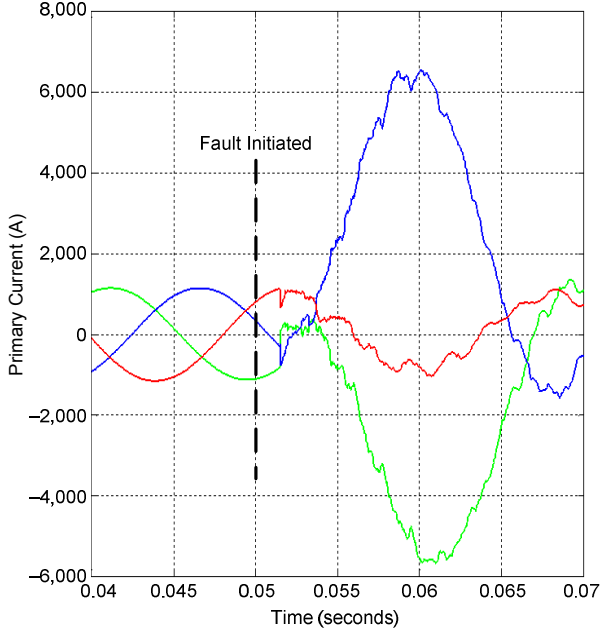

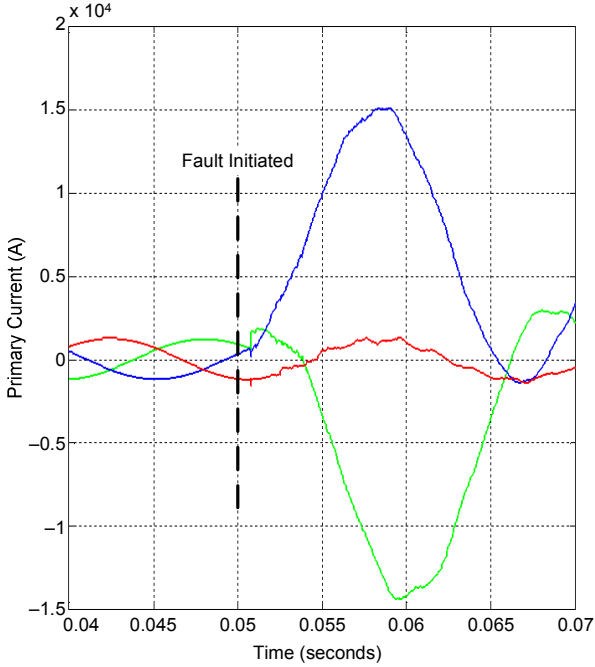Fig. 13. Phase currents applied to the sending-end terminal for an AB fault.

Fig. 14. Phase currents applied to the receiving-end terminal for an AB fault.

The relays filter the phase currents to capture the high-frequency content of the signals. The relays exchange the time stamp of the retrieved high-frequency wave. Fig. 15 and Fig. 16 show the high-frequency content of the phase currents that were retrieved from the relays.
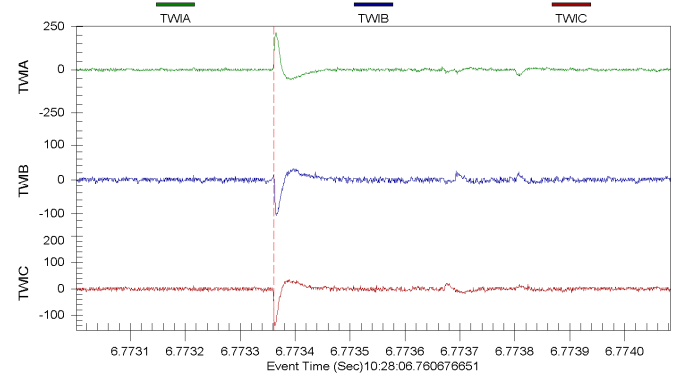

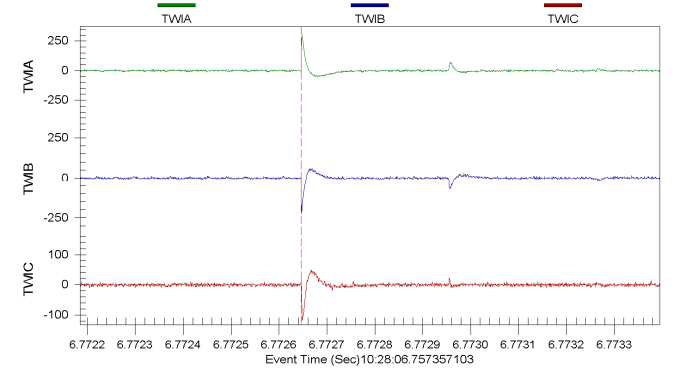Fig. 15. TWs captured at the sending end for an AB fault.

Fig. 16. TWs captured at the receiving end for an AB fault.

We calculated the TW propagation velocity using the TW information obtained for a line energization event.

The relays recorded the following left terminal (TwaveL) and right terminal (TwaveR) time stamps for this event:

- TwaveL = 6.773364044 seconds
- TwaveR = 6.772648441 seconds
- LL = 189 miles
- LPVEL = 0.9903
- c = 186282.39705 miles per second

The distance to the fault is 160.51 miles, as shown in (12).

In this case, the fault location estimation error is 0.06 miles.

$$D_{Fault} = \frac{189 \text{ miles}}{2} + \frac{0.9903 \bullet 186,282.39705 \text{ miles/s} \bullet (6.773364044 - 6.772648441)}{2}$$
$$D_{Fault} = 160.51 \text{ miles}$$

(12)

B. Testing Using a Physical Line Model

Additional verification was performed using the physical single-phase transmission line model shown in Fig. 17. Although less precise and significantly less versatile than EMTP simulations, the physical low-energy transmission line model offered the ability to test the entire system (including the relay input CTs).
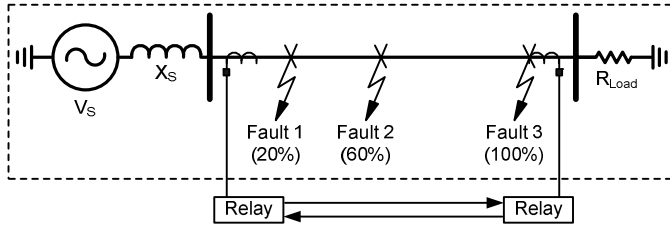

Fig. 17. Physical transmission line model.

The physical transmission line model was implemented using a total of 500 π sections to simulate a 38-mile line. The custom card developed for this model is shown in Fig. 18. The model operates at 48 V, 1 A with a maximum fault current level of 5 A. Faults can be applied at three locations. Fig. 17 shows faults at 20, 60, and 100 percent of the line length.
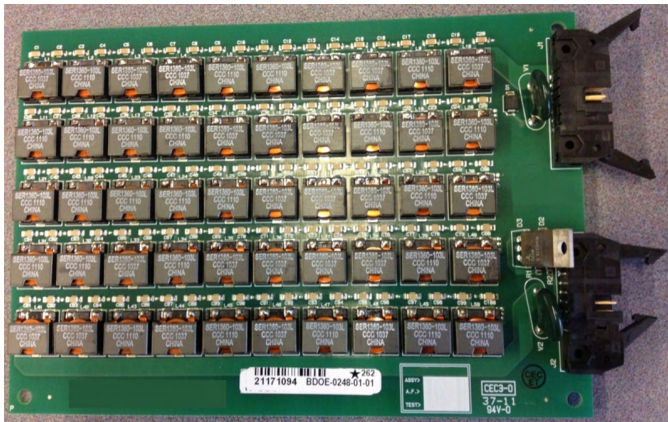

Fig. 18. Transmission line model section used to simulate a 3.8-mile single-phase segment. The thyristor-based fault model is visible at the lower right-hand side. The complete line model uses 10 sections.

VI. FIELD INSTALLATION

A. Fault Location Experience

BPA owns and operates Goshen and Drummond substations. The Goshen-Drummond line is operated at 161 kV, and according to the BPA system data book, its line length is 72.77 miles. This transmission line is located in eastern Idaho close to the Wyoming border (see Fig. 19). The line shares a right of way with two other 161 kV lines for approximately 4.75 miles. Then it shares the right of way with

another 161 kV line for the next 17 miles. The line was originally built for 115 kV and was later upgraded to 161 kV without changing conductors or insulators.
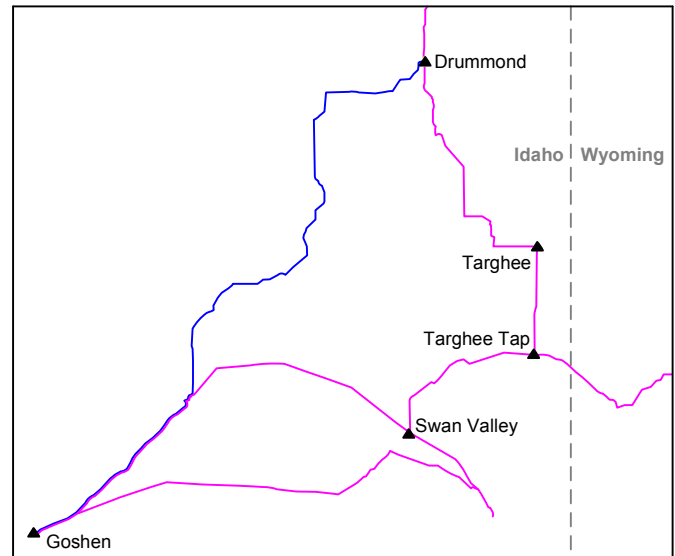

Fig. 19. Goshen-Drummond 161 kV line (blue) and neighboring 161 kV lines (magenta).

After the 161 kV upgrade, the line experienced 40 faults in the past five years. The most common causes of faults on this line include the following:

- Galloping conductors clashing because of the wind.
- Farmers spraying fertilizers on the conductors and insulators.
- Flying projectiles hitting the conductors and insulators.

In the past, for a permanent fault, a lineman would drive along the line until the fault was found. For a long line built over rough terrain, this approach could cause a long outage. Later, BPA used oscillographic records of faults to estimate the fault location. BPA personnel calculated the impedance to the fault from the fault voltages and currents and estimated the fault location. This information would give the lineman a starting point to look for the fault. For temporary faults, linemen inspected every insulator looking for an indication of where the flash occurred. With the advent of digital relays, the relay would estimate the fault location based upon the impedance and the length of the line. If either of these were not accurate, then the location would not be accurate. Multiple sections, different tower configurations, fault resistance, system nonhomogeneity, and zero-sequence mutual coupling challenge the accuracy of impedance-based fault locating methods.

The Goshen-Drummond line is composed of four different tower structures, as shown in Fig. 20. The line is spanned across 18 sections. Table II shows the tower type and line length associated with each section.
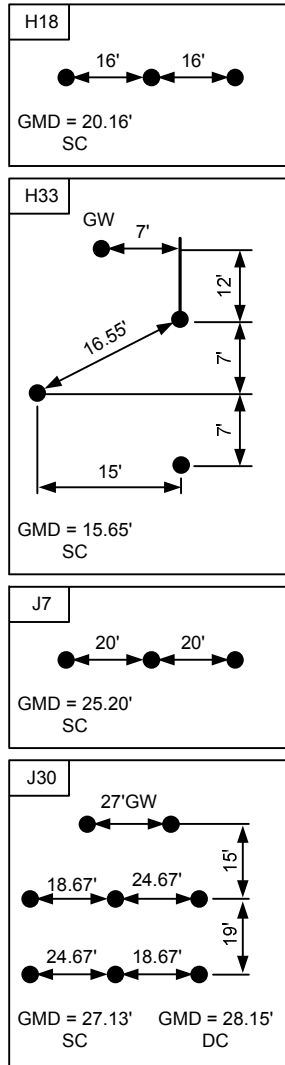

Fig. 20. Tower structures on the Goshen-Drummond line.

TABLE II
TOWER TYPE AND LINE SECTION LENGTH

Tower Type	Length (miles)
H18	0.12
J30	21.05
J7	0.68
H33	11.63
J7	0.52
J7	0.25
J7	0.94
H33	2.22
J7	4.08
J30	0.79
J30	0.42
J30	0.08
J7	8.86
H33	5.41
J7	0.37
J7	1.27
H33	5.82
J7	8.27

Fig. 21 shows the one-line diagram that includes the Goshen-Drummond line and relay CT connections. Notice that the line termination at Drummond is an autotransformer.
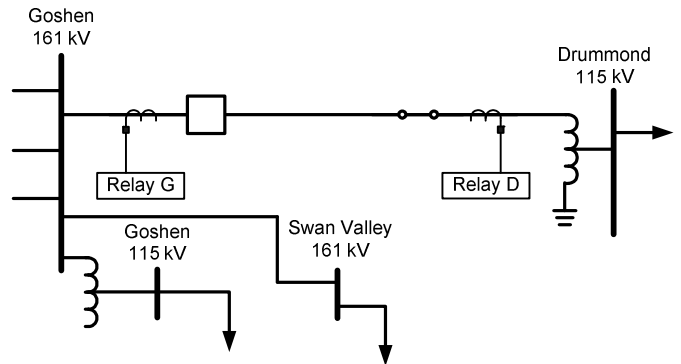

Fig. 21. Transmission network that includes the Goshen-Drummond line.

B. Traveling Wave Device Installation

On April 4, 2012, BPA installed two relays with TW locating capability on the Goshen-Drummond 161 kV line. These relays are capable of exchanging TW information via a 64 kbps channel and estimating fault location in real time, but the communications channels were not available at installation. Therefore, we manually retrieved the COMTRADE event records with TW information and estimated the fault location after the occurrence of each fault. The event records include the TW phase currents and time-stamp information.

C. Propagation Velocity and Line Length

As previously mentioned, double-end TW fault location relies on the line length and propagation velocity settings along with the measured time difference between the arrival times of the TWs captured at both terminals of the transmission line. Typically, utilities have an estimate of the line length based on the geographic or linear length or "road miles" of the transmission line; some utilities consider line sag in their estimates. Including the sag in line length estimates reduces errors in the TW fault location.

We measured the propagation velocity based on the line length and travel time of the waves. We estimated travel time using the TW information that we captured during line energization. We energized the line from Goshen while the terminal at Drummond was open and captured the event reports to determine the wave propagation velocity. Fig. 22 shows the phase currents and voltages captured at the Goshen terminal sampled at 8 kHz.
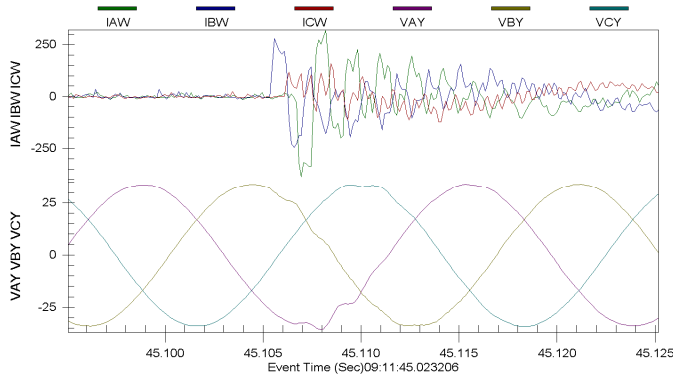

Fig. 22.   Phase voltages and currents captured during line energization from Goshen.

The phase currents depicted in Fig. 22 show the pole scatter and the sequence of pole closing: B-phase, C-phase, and A-phase. Furthermore, we can observe that the B-phase and A-phase poles closed near the peak of their corresponding voltages, while the C-phase pole closed near the voltage zero crossing. Fig. 23 shows the phase currents filtered using an analog band-pass filter, preserving the high-frequency content and rejecting the fundamental frequency content; the currents are sampled at 1.56 MHz.
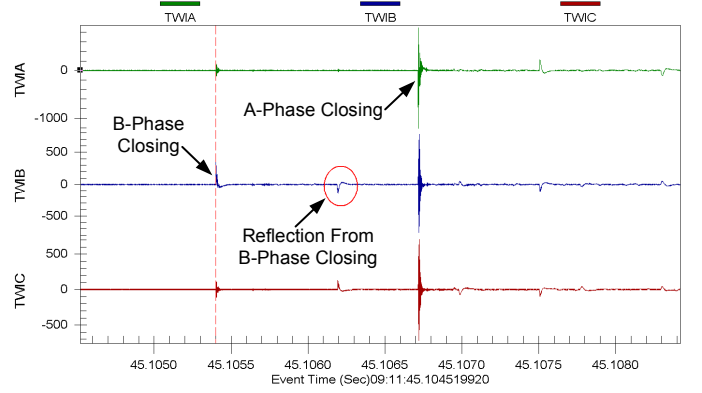

Fig. 23.   TW phase currents captured during line energization.

Fig. 23 shows that there is no detectable transient corresponding to the C-phase closing as the pole closed at near voltage zero. The information in Fig. 23 can be used to determine the pole scatter among the breaker contacts accurately to hundreds of nanoseconds. This information can be further used to determine if corrective breaker maintenance is needed. We used the time stamps corresponding to B-phase pole closing and the reflected wave from the open terminals to calculate the propagation velocity. We show the propagation velocity calculations in (13) and (14), with travel time equal to 790.605 microseconds and line length equal to 72.77 miles.

$$LPVEL = \frac{2 \cdot LL}{\text{Travel time}} \cdot \frac{1}{c} \tag{13}$$

$$LPVEL = \frac{2 \cdot 72.77 \text{ miles}}{790.605 \text{ μs}} \cdot \frac{1}{186282.39705 \text{ miles/s}} \tag{14}$$

$$= 0.98821$$

D. Power System Faults and Fault Location Estimates

1) Event 1: C-Phase-to-Ground Fault

The first fault occurred on April 24, 2012. Fig. 24 and Fig. 25 show the TWs captured at the Goshen and Drummond terminals for the C-phase-to-ground fault.
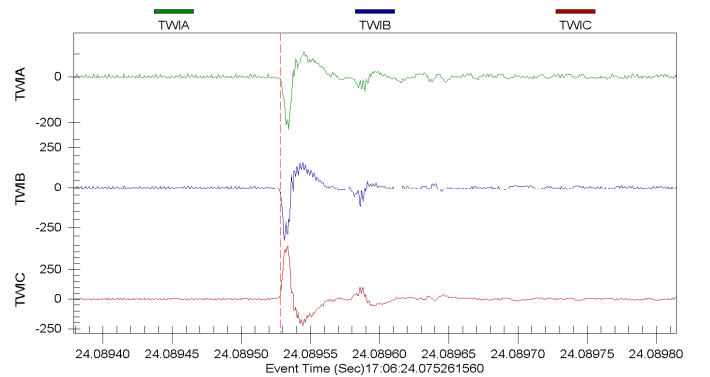

Fig. 24.   Phase currents at Goshen for the C-phase-to-ground fault at 67.91 miles from Goshen terminal.
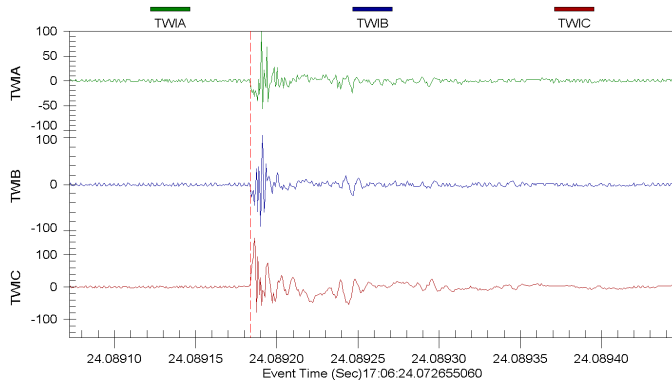
Fig. 25.   Phase currents at Drummond for the C-phase-to-ground fault at 67.91 miles from Goshen terminal.

The time stamps corresponding to the TW arrival obtained from the event records include the following:

- Goshen: Twave$_{Gosh}$ = 24.089532202 seconds
- Drummond: Twave$_{Drum}$ = 24.089186645 seconds

Based on the measured TW arrival times, we estimated from (11) a fault location of 68.19 miles from the Goshen terminal. When the line crew patrolled the line, they found a damaged insulator at 67.91 miles from the Goshen terminal. Fig. 26 shows the damaged insulator. The line crew reported that the cause of the insulator damage could be a flashover.

Fig. 26.   Damaged insulator at 67.91 miles from Goshen terminal.

2) Event 2: B-Phase-to-Ground Fault

The second fault occurred on May 11, 2012. This permanent fault was caused by a lead projectile hitting the B-phase insulators at a high speed. Fig. 27 and Fig. 28 show the high-frequency components of the phase currents captured at both terminals.
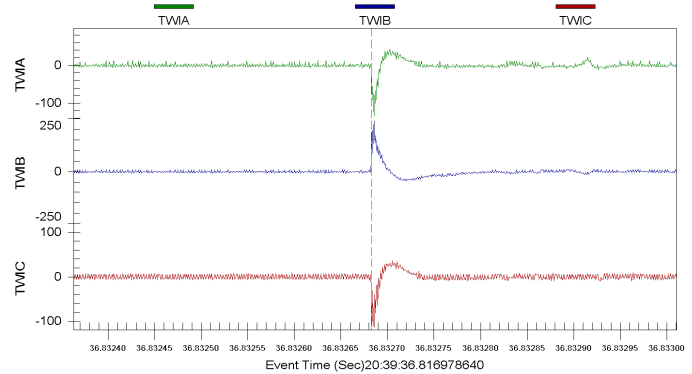

Fig. 27.   Phase currents at Goshen for the B-phase-to-ground fault at 38.16 miles from the Goshen terminal.

Fig. 28.   Phase currents at Drummond for the B-phase-to-ground fault at 38.16 miles from the Goshen terminal.

The time stamps corresponding to the TW arrival obtained from the event records include the following:

- Goshen: Twave$_{Gosh}$ = 36.832684476 seconds
- Drummond: Twave$_{Drum}$ = 36.832667109 seconds

We estimated a fault location of 37.98 miles from the Goshen terminal. The line crew found the fault at 38.16 miles from the Goshen terminal. Fig. 29 shows one of the damaged insulators in the insulator string.

Fig. 29.   Damaged insulator at 38.16 miles from the Goshen terminal.

3) Event 3: B-Phase-to-Ground Fault

The third fault was on May 26, 2012. Fig. 30 and Fig. 31 show the high-frequency components of the phase currents captured at both terminals.

Fig. 30. Phase currents at Goshen for the B-phase-to-ground fault at 66.86 miles from the Goshen terminal.
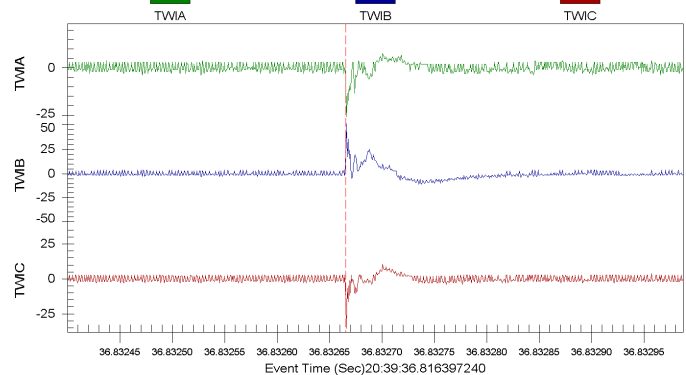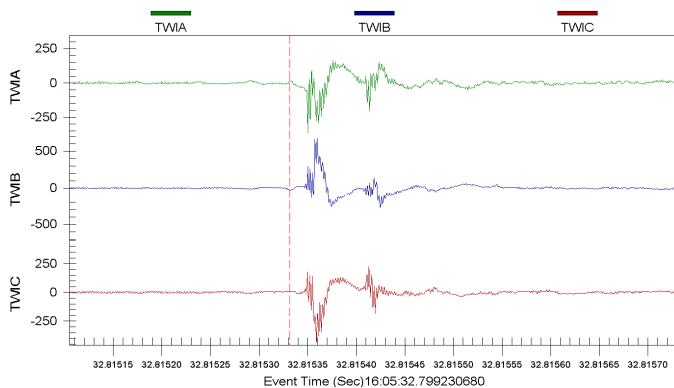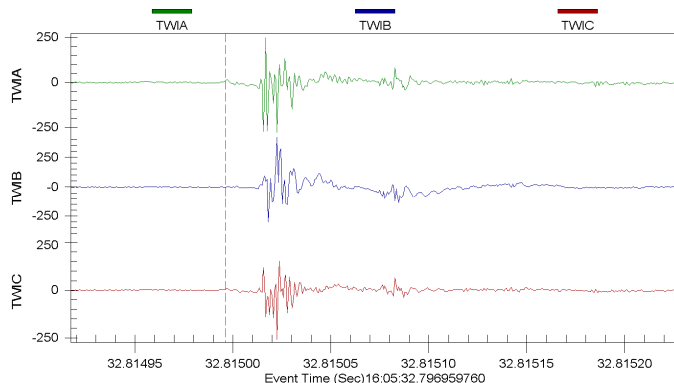

Fig. 31. Phase currents at Drummond for the B-phase-to-ground fault at 66.86 miles from the Goshen terminal.

Based on the prestrikes recorded at the Goshen terminal, it is suspected that the fault was due to lightning. The time stamps corresponding to the TW arrival obtained from the event records include the following:

- Goshen: $Twave_{Gosh}$ = 32.815358756 seconds
- Drummond: $Twave_{Drum}$ = 32.815023378 seconds

We estimated a fault location of 67.25 miles from the Goshen terminal. The line crew found the fault at 66.86 miles from Goshen.

4) Summary of Results

Table III provides the fault location reported by the relay based on TW measurements and the actual fault location reported by BPA. The errors between the TW-based estimated distances and the BPA reported distances are attributed to the nonuniformity of the line sag due to terrain elevation changes and differences in tower structures. BPA is working on providing accurate line length estimates to include line sag.

TABLE III
REPORTED FAULT LOCATIONS AND ASSOCIATED ERRORS

Event Number	Faulted Phase	TW-Based Estimated Distance	BPA Reported Distance	Error
1	C	68.19 miles	67.91 miles	0.28 miles
2	B	37.98 miles	38.16 miles	–0.18 miles
3	B	67.25 miles	66.86 miles	0.39 miles

VII. CONCLUSION

Adding TW-based fault location to line protective relays improves their fault locating capability compared with relays that use only impedance-based fault locating methods.

Relays that use TWs and impedance-based methods to estimate fault location provide results independent of the fault incidence angle. These relays provide fault location at the line terminals within a couple of seconds without the need for an additional computer and software.

Field cases demonstrate that relays with TW fault locating capability can locate faults to within a tower span in applications including lines with mutual coupling. Furthermore, there is no need for additional secondary wiring and communications equipment when TW-based fault location is part of the line differential relay.

VIII. REFERENCES

[1] T. W. Stringfield, D. J. Marihart, and R. F. Stevens, "Fault Location Methods for Overhead Lines," *Transactions of the American Institute of Electrical Engineers – Part III: Power Apparatus and Systems*, Vol. 76, Issue 3, April 1957, pp. 518–530.

[2] D. J. Marihart and N. W. Haagenson, "Automatic Fault Locator for Bonneville Power Administration," proceedings of the 1972 IEEE Power and Energy Society Summer Meeting, San Francisco, CA, July 1972.

[3] M. Ando, E. O. Schweitzer, III, and R. A. Baker, "Development and Field-Data Evaluation of Single-End Fault Locator for Two-Terminal HVDC Transmission Lines, Part I: Data Collection System and Field Data," *IEEE Transactions on Power Apparatus and Systems*, Vol. PAS–104, Issue 12, December 1985, pp. 3524–3530.

[4] M. Ando, E. O. Schweitzer, III, and R. A. Baker, "Development and Field-Data Evaluation of Single-End Fault Locator for Two-Terminal HVDC Transmission Lines, Part II: Algorithm and Evaluation," *IEEE Transactions on Power Apparatus and Systems*, Vol. PAS–104, Issue 12, December 1985, pp. 3531–3537.

[5] M. A. Street, "Delivery and Application of Precise Timing for a Traveling Wave Powerline Fault Locator System," proceedings of the 22nd Annual Precise Time and Time Interval (PTTI) Applications and Planning Meeting, Vienna, VA, December 1990, pp. 355–360.

[6] P. F. Gale, "Overhead Line Fault Location Based on Travelling Waves and GPS," proceedings of the Precise Measurements in Power Systems Conference, Arlington, VA, October 1993.

[7] M. Aurangzeb, P. A. Crossley, and P. Gale, "Fault Location on a Transmission Line Using High Frequency Travelling Waves Measured at a Single Line End," proceedings of the 2000 IEEE Power Engineering Society Winter Meeting, Vol. 4, Singapore, January 2000, pp. 2437–2442.

[8] D. A. Tziouvaras, J. Roberts, and G. Benmouyal, "New Multi-Ended Fault Location Design for Two- or Three-Terminal Lines," proceedings of the 7th International Conference on Developments in Power System Protection, Amsterdam, Netherlands, April 2001.

[9] K. Zimmerman and D. Costello, "Impedance-Based Fault Location Experience, " proceedings of the 31st Annual Western Protective Relay Conference, Spokane, WA, October 2004.

[10] B. S. Guru and H. R. Hiziroglu, *Electromagnetic Field Theory Fundamentals*. PWS Publishing Company, Boston, MA, June 1997.

[11] P. Moreno, P. Gómez, J. L. Naredo, and J. L. Guardado, "Frequency Domain Transient Analysis of Electrical Networks Including Non-linear Conditions," *International Journal of Electrical Power & Energy Systems*, Vol. 27, Issue 2, February 2005, pp. 139–146.

[12] D. E. Hedman, "Propagation on Overhead Transmission Lines I: Theory of Modal Analysis," *IEEE Transactions on Power Apparatus and Systems*, Vol. 84, Issue 3, March 1965, pp. 200–205.

[13] S. A. Schelkunoff, "The Electromagnetic Theory of Coaxial Transmission Lines and Cylindrical Shields," *The Bell System Technical Journal*, Vol. 13, No. 4, October 1934, pp. 532–579.

[14] D. Hou and J. Roberts, "Capacitive Voltage Transformers: Transient Overreach Concerns and Solutions for Distance Relaying," proceedings of the 22nd Annual Western Protective Relay Conference, Spokane, WA, October 1995.

[15] E. O. Schweitzer, III, "Evaluation and Development of Transmission Line Fault-Locating Techniques Which Use Sinusoidal Steady-State Information," proceedings of the 9th Annual Western Protective Relay Conference, Spokane, WA, October 1982.

[16] T. Takagi, Y. Yamakoshi, M. Yamaura, R. Kondow, and T. Matsushima, "Development of a New Type Fault Locator Using the One-Terminal Voltage and Current Data," *IEEE Transactions on Power Apparatus and Systems*, Vol. PAS–101, Issue 8, August 1982, pp. 2892–2898.

[17] B. Kasztenny, B. Le, and N. Fischer, "A New Multiterminal Fault Location Algorithm Embedded in Line Current Differential Relays," proceedings of the 11th International Conference on Developments in Power System Protection, Birmingham, UK, April 2012.

[18] H. Lee, "Development of an Accurate Travelling Wave Fault Locator Using the Global Positioning System Satellites," proceedings of the 20th Annual Western Protective Relay Conference, Spokane, WA, October 1993.

[19] D. A. Douglass, "Current Transformer Accuracy With Asymmetric and High Frequency Fault Current," *IEEE Transactions on Power Apparatus and Systems*, Vol. 100, Issue 3, March 1981, pp. 1006–1012.

[20] M. A. Redfern, S. C. Terry, F. V. P. Robinson, and Z. Q. Bo, "A Laboratory Investigation Into the use of MV Current Transformers for Transient Based Protection," proceedings of the 2003 International Conference on Power Systems Transients (IPST), New Orleans, LA, September–October 2003.

[21] A. M. Elhaffar, "Power Transmission Line Fault Location Based on Current Traveling Waves," doctoral dissertation, Helsinki University of Technology, Finland, March 2008.

[22] D. J. Spoor, J. Zhu, and P. Nichols, "Filtering Effects of Substation Secondary Circuits on Power System Traveling Wave Transients," proceedings of the 8th International Conference on Electrical Machines and Systems (ICEMS), Vol. 3, September 2005, pp. 2360–2365.

[23] M. Kezunovic, L. Kojovic, V. Skendzic, C. W. Fromen, D. Sevcik, and S. L. Nilsson, "Digital Models of Coupling Capacitor Voltage Transformers for Protective Relay Studies," *IEEE Transactions on Power Delivery*, Vol. 7, Issue 4, October 1992, pp. 1927–1935.

[24] L. V. Bewley, *Traveling Waves on Transmission Systems*. Dover Publications, Mineola, NY, 1963.

IX. BIOGRAPHIES

Stephen Marx received his BSEE from the University of Utah in 1988. He joined Bonneville Power Administration (BPA) in 1988. He is presently the District Engineer in Idaho Falls, Idaho, for BPA. He has over 25 years of experience in power system protection and metering. He has been a lecturer at the Hands-On Relay School in Pullman, Washington, since 2007. He is a registered professional engineer in the state of Oregon. He is a member of IEEE and has authored and coauthored several technical papers.

Brian K. Johnson received a Ph.D. degree in electrical engineering from the University of Wisconsin-Madison in 1992. He is currently a professor in the ECE Department at the University of Idaho, Moscow. His interests include power electronics, power system protection, and modeling and simulation of power system transients. Dr. Johnson is a professional engineer in the state of Idaho.

Armando Guzmán received his BSEE with honors from Guadalajara Autonomous University (UAG), Mexico. He received a diploma in fiber-optics engineering from Monterrey Institute of Technology and Advanced Studies (ITESM), Mexico, and his MSEE and MECE from the University of Idaho, USA. He served as regional supervisor of the Protection Department in the Western Transmission Region of the Federal Electricity Commission (the Mexican electrical utility company) in Guadalajara, Mexico, for 13 years. He lectured at UAG and the University of Idaho in power system protection and power system stability. Since 1993, he has been with Schweitzer Engineering Laboratories, Inc., in Pullman, Washington, where he is a fellow research engineer. He holds numerous patents in power system protection and metering. He is a senior member of IEEE.

Veselin Skendzic is a principal research engineer at Schweitzer Engineering Laboratories, Inc. He earned his BS in electrical engineering from FESB, University of Split, Croatia; his Masters of Science from ETF, Zagreb, Croatia; and his Ph.D. from Texas A&M University. He has more than 25 years of experience in electronic circuit design and power system protection-related problems. He is a senior member of IEEE, has written multiple technical papers, and is actively contributing to IEEE and IEC standard development. He is a member of the IEEE Power Engineering Society (PES) and the IEEE Power System Relaying Committee (PSRC) and a past chair of the PSRC Relay Communications Subcommittee (H).

Mangapathirao (Venkat) Mynam received his MSEE from the University of Idaho in 2003 and his BE in electrical and electronics engineering from Andhra University College of Engineering, India, in 2000. He joined Schweitzer Engineering Laboratories, Inc. (SEL) in 2003 as an associate protection engineer in the engineering services division. He is presently working as a lead research engineer in SEL research and development. He was selected to participate in the U.S. National Academy of Engineering (NAE) 15th Annual U.S. Frontiers of Engineering Symposium. He is a senior member of IEEE.